Journal of Applied Electrochemistry **29**: 497–503, 1999.

Electrochemical reduction of trivalent uranium ions in molten chlorides

K. SERRANO and P. TAXIL*
Laboratoire de Génie Chimique, U.M.R. 5503, 118 route de Narbonne, 31062 Toulouse, Cedex 04, France
*(*author for correspondence)*

Received 20 March 1998; accepted in revised form 1 September 1998

Key words: chronopotentiometry, electrochemical reduction, molten chlorides, square wave voltammetry, uranium

Abstract

The electrochemical behaviour of U^{III} in molten salts was studied at 715 °C under argon atmosphere in a molten equimolar NaCl–KCl mixture containing uranium ions in oxidation state III (UCl_3). Three different complementary electrochemical methods were used, namely cyclic voltammetry, chronopotentiometry and square wave voltammetry. These techniques provide data to explain the electroreduction mechanism. The reduction of U^{III} in the NaCl–KCl mixture occurs in a single step with an exchange of three electrons, this process is controlled by the diffusion of U^{III}. The diffusion coefficient of U(III) was calculated using the three electrochemical methods.

1. Introduction

Electrochemical studies on uranium in molten salts began in the 1960s: at that time, Smirnov et al. [1] and Boisde et al. [2] investigated the electrolysis of NaCl–KCl mixtures containing UCl_3, UCl_4 and UO_2Cl_2, with similar results. Based on their own measurements of UCl_3 polarization curves, using cyclic voltammetry, they claimed that metallic uranium is deposited on the cathode from U^{3+} ions as a result of a reversible single reduction step involving the exchange of three electrons.

The potential of the U(III)/U(0) couple in molten chloride salts has been measured by several authors; in particular Flengas [3] found $E = -1.43\,V$ vs Ag/AgCl (5×10^{-2} mol mol^{-1}) in NaCl–KCl–UCl_3 (8.3×10^{-3} mol mol^{-1}). All data concerning potential measurements have been reviewed by Partridge [4].

References [5–9] deal with the measurement of the diffusion coefficient $D_{U(III)}$, in various molten melts (LiCl–KCl, LiCl–CsCl, RbCl–CsCl, NaCl–KCl, NaCl–$AlCl_3$ and LiCl–NaCl–$CaCl_2$–$BaCl_2$). Some disagreements between these authors were noticed since the values of $D_{U(III)}$ lie between 2.5 and 49×10^{-6} cm^2 s^{-1}.

This paper describes a study of the electrochemical reduction of uranium ions in chloride melt. The main aim is to identify the stages of reduction leading to uranium metal, that is, the number of steps and the number of electrons exchanged at each step.

2. Experimental process

Technical details on the cell used may be found elsewhere [10]. The electrolytic bath was composed of an equimolar mixture of NaCl and KCl as solvent and UCl_4 as solute. Granules of uranium metal, always kept in excess, were placed in the crucible in order to produce trivalent uranium according to the following reaction:

$$3\,UCl_4 + U \rightarrow 4\,UCl_3$$

Uranium tetrachloride was introduced through an airlock into the melt under argon. The bath was initially dehydrated by heating the mixture of salts up to its melting point (658 °C) under vacuum (4×10^{-2} mbar).

The electrolyte was contained in a vitreous carbon crucible placed in a graphite chamber inside a cylindrical refractory steel chamber; this arrangement prevents the attack of the inside wall of the chamber by molten salt vapours [10]. The cell was closed by a water-cooled stainless steel lid. The experiments were performed in an inert atmosphere of grade U argon previously dehydrated and deoxygenated using a purification cartridge (Air liquide).

The working and reference electrodes were 1 mm diameter wires of tungsten (dipped 1 cm into the bath) and platinum, respectively. The potential of the platinum wire is fixed by the Pt(II)/Pt system [11]. The

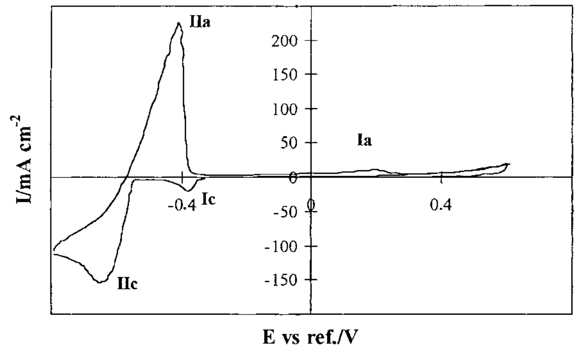

Fig. 1. Cyclic voltammogram of NaCl–KCl–UCl$_3$ (2 mass %), $\theta = 700\,°C$, $S = 0.492\ cm^2$, $v = 200\ mV\,s^{-1}$. Working electrode W, comparison electrode Pt; counter electrode vitreous carbon.

auxiliary electrode was a vitreous carbon rod with a large surface area ($2\ cm^2$).

Three electrochemical methods were used; namely, cyclic voltammetry, chronopotentiometry and square wave voltammetry.

3. Results and discussion

3.1. *Cyclic voltammogram of the NaCl–KCl–UCl$_3$ mixture*

A typical cyclic voltammogram of the reduction of U(III) in equimolar NaCl–KCl at 700 °C on a tungsten electrode is shown in Figure 1. It exhibits one IIc peak and a Ic prepeak associated with anodic peaks IIa and Ia, respectively, observed after reverse scanning.

3.2. *Investigation of prepeak Ic*

We observed that the presence and the position of prepeak Ic depend both on the nature of the working electrode and its surface state:

(i) When this electrode is silver, iron, copper, molybdenum or vitreous carbon, prepeak Ic is observed at more anodic potentials than peak IIc, whereas it is more cathodic (postpeak) when platinum is used as working electrode.

(ii) Prepeak Ic is no longer observed when the product of the reaction associated with this peak is not removed by anodic polarization.

(iii) The relationship between the current density of prepeak i_{pIc} and the uranium ion content, [U], is reported in Figure 2. i_{pIc} increases with [U] at low concentrations and remains constant when [U] exceeds 2% weight. The shape of this curve indicates that peak Ic obeys a Langmuir adsorption relationship. An adsorption mechanism is indicated by consideration of the model of the formation of a thin layer nonlimited by the mass transfer on the electrode; this model [12] predicts that Equation 1 is verified, in the increasing part of the $i_{pIc}/\sqrt{v} = f([U])$ relationship:

$$\frac{i_{pIc}}{v} = \frac{n^2F^2lC_0}{4RT} \tag{1}$$

where l is the thickness of the layer and C_0 the concentration of the electroactive species. The data reported in Table 1 obey Equation 1. Furthermore

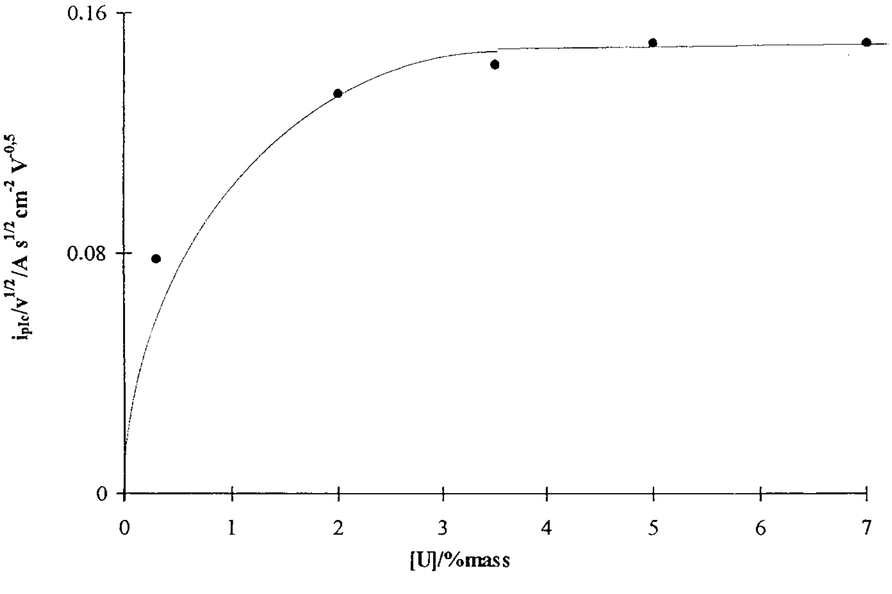

Fig. 2. i_{pIc} against [U] , $\theta = 690\,°C$. Working electrode W, comparison electrode Pt.

Table 1. Different values of the ratio i_{pIc}/v of the prepeak Ic for different scan rates v

i_{pIc}/A cm^{-2}	v/V s^{-1}	(i_{pIc}/v)/A s V^{-1} cm^{-2}
0.100	0.6	0.163
0.115	0.7	0.165
0.132	0.8	0.165
0.137	0.9	0.152
0.166	1	0.166

θ = 690 °C, working electrode W.

the average value of i_{pIc}/v allows the thickness of the layer to be calculated as $l = 4\ \mu$m.

Reverse chronopotentiometric runs (shown in Figure 3) confirm the formation of an insoluble compound on the electrode, since the anodic transition time τ_{Ia} is found to be equal to the cathodic transition time τ_{Ic}. The number of electrons in this step can be calculated by using Equation [2] in the cathodic part of Figure 3 [13]:

$$E = \frac{RT}{nF}\ln\left(\frac{\tau_{\mathrm{Ic}} - t}{t}\right) \tag{2}$$

The slope of the straight line $E = f[\ln(\tau_{Ic} - t)/t]$ in Figure 4 leads to $n = 2.3$ (≈ 2).

Thus, it can be concluded that peak Ic is associated with adsorption

$$\mathrm{U^{III}} + 2\,\mathrm{e^-} \rightarrow \mathrm{U^I}$$

leading to the formation of a monovalent and insoluble compound of uranium adsorbed on the electrode. Note that in other chloride media, Martinot observed the formation of uranium subhalide with higher valency [14].

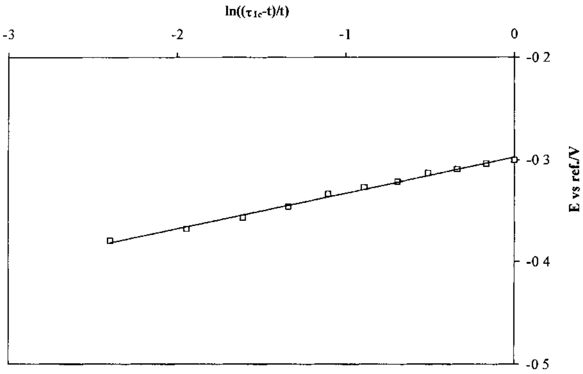

Fig. 4. E against $\ln((\tau_{\mathrm{Ic}} - t)/t)$ of $\mathrm{UCl_3}$ in NaCl–KCl, $i = 35.5$ mA cm^{-2}, $\theta = 715$ °C. Working electrode W; comparison electrode Pt.

3.3. *Analysis of peak IIc*

Reverse chronopotentiometric measurements, Figure 5, showed that the ratio $\tau_{\mathrm{IIc}}/\tau_{\mathrm{IIa}}$ equals one (Table 2), which is characteristic of the formation of an insoluble product.

3.3.1. *Determination of the number of electrons exchanged in peak IIc.*

For this purpose the numerical results from cyclic voltammetry, chronopotentiometry and square wave voltammetry were combined.

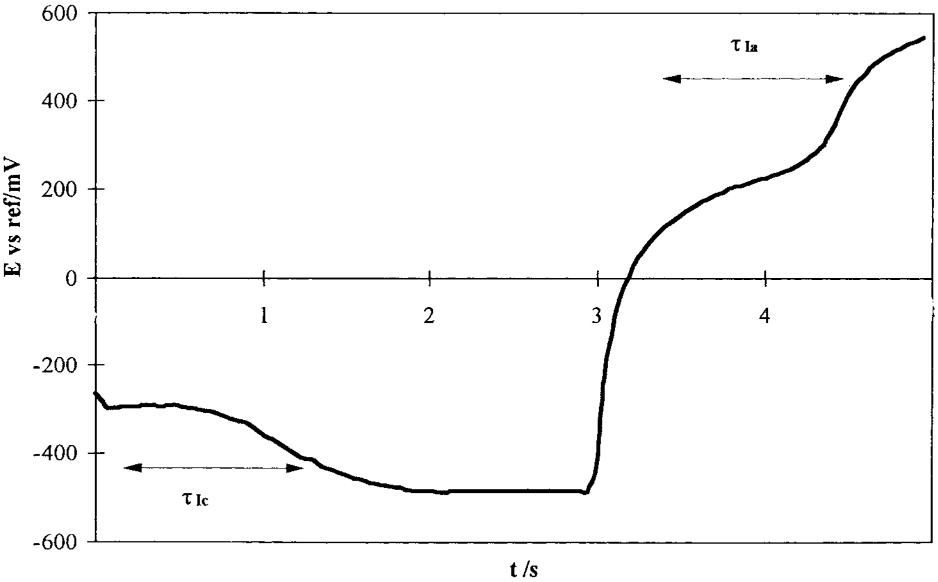

Fig. 3. Reversal chronopotentiogram of $\mathrm{UCl_3}$ in NaCl–KCl, $i = 35.5$ mA cm^{-2}, $\theta = 715$ °C. Working electrode W; comparison electrode Pt.

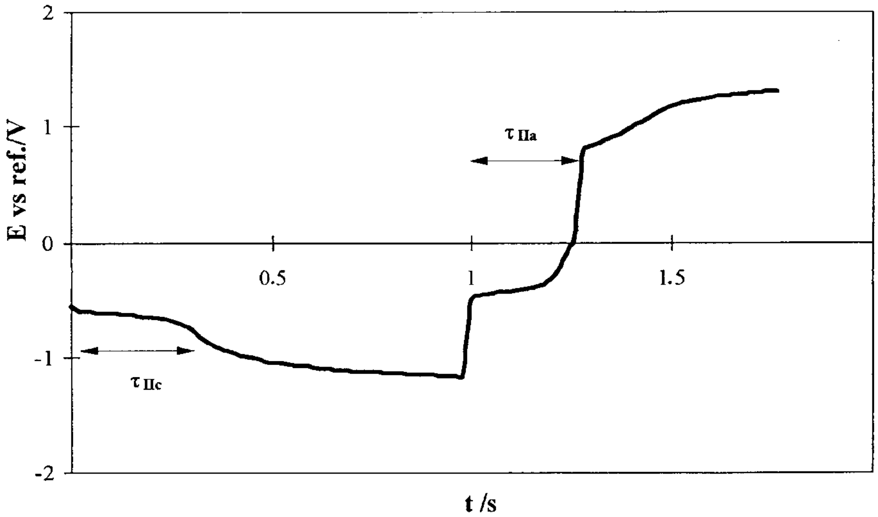

Fig. 5. Reversal chronopotentiogram of UCl_3 in NaCl–KCl, $i = 169\,mA\,cm^{-2}$, $\theta = 715\,°C$, [U] = 1.5 mass %. Working electrode W.

Table 2. Different values of the ratio τ_{IIc}/τ_{IIa} of the peak IIc for different current densities i

i/mA cm^{-2}	τ_{IIc}/s	τ_{IIa}/s	τ_{IIc}/τ_{IIa}
−84.5	0.74	0.74	1
−169.0	0.32	0.3	1.07
−225.3	0.16	0.17	0.94
−281.7	0.11	0.11	1

(a) *Cyclic voltammetry and chronopotentiometry*

The peak current i_{pIIc} is found to change linearly with the square root of scanning rate v on the tungsten electrode as shown in Figure 6. It can be concluded that this step is controlled by the diffusion of the electroactive species at the electrode surface. Due to the reversibility of the U^{III}/U^0 system [1, 2], confirmed by the low potential difference between the direct and reverse curves, we can use the Randles–Sevick equation [15]:

$$\frac{i_p}{\sqrt{v}} = 0.61\,(nF)^{3/2}(RT)^{-1/2}D^{1/2}C_0 \qquad (3)$$

where n is the number of electrons involved in the reaction, F is the faradaic constant, R is the gas constant

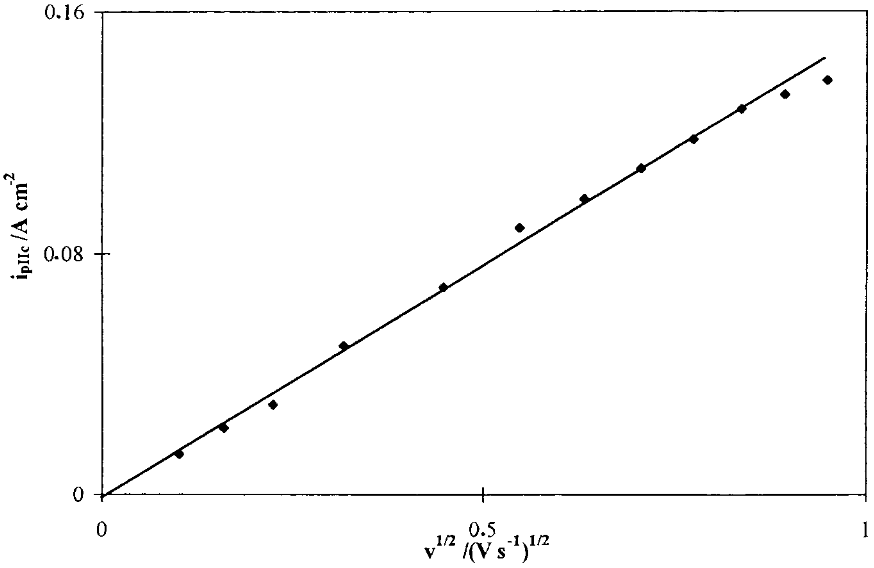

Fig. 6. Current of peak IIc against the square root of the scan rate v, $\theta = 715\,°C$, [U] = 1.5 mass %. Working electrode W (0.5 cm^2); comparison electrode Pt.

(8.314 J mol^{-1} K^{-1}), T is the temperature in kelvin and C_0 is the bulk concentration of the electroactive species (mol cm^{-3}).

Furthermore, additional results were obtained from chronopotentiometric runs, as seen in Figure 7, the product $i\sqrt{\tau}$ does not depend on i; thus, the Sand equation is verified [16]:

$$i\sqrt{\tau} = 0.5\,\pi^{1/2} nFC_0 D^{1/2} \tag{4}$$

Combining Equations 1 and 2 gives $(i_{\mathrm{pIc}}/\sqrt{v})/i\sqrt{\tau} = K\sqrt{n}$ with $K = 41.95/\sqrt{T}$ and allows the number of electrons to be calculated. As seen in Table 3, three electrons are exchanged at various temperatures between 680 °C and 716 °C.

(b) *Square wave voltammetry*

This result is confirmed by square wave voltammetry. In Figure 8, we observed the square wave voltammogram of a solution of UCl_3, plotted in the cathodic potential range (from −0.4 to −1 V). According to [17], in the case of a single step, the signal must be Gaussian shaped. In Figure 8, the observed peak is asymmetric; this may be attributed to the following:

(i) The nucleation overpotential which delays the rise of the current [18].

(ii) The compactness of the film formed by adsorbed species renders the reduction more difficult. Additional energy is required to overcome this barrier [19].

Thus, the shape of this peak may be due to a 'deblocking' effect.

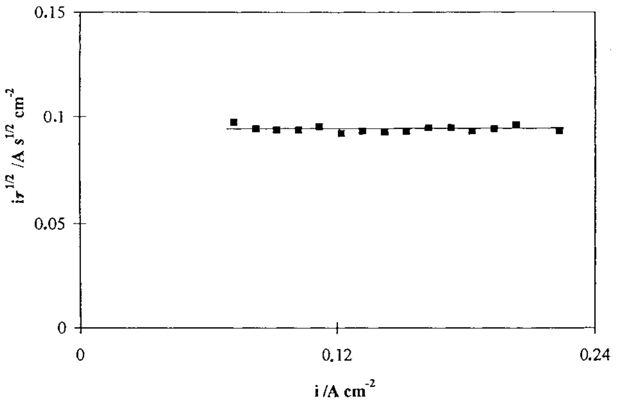

Fig. 7. $i\sqrt{\tau}$ against i, $\theta = 715\,°C$, [U] = 1.5 mass %. Working electrode W; comparison electrode Pt.

Table 3. Number of electrons exchanged, n, at different temperatures calculated by combining cyclic voltammetry and chronopotentiometry

θ/°C	$i/\sqrt{v}$/A cm^{-2} s$^{1/2}$ V$^{-1/2}$	$i\tau^{1/2}$/A cm^{-2} s$^{1/2}$	n
716	0.39	0.17	2.97
700	0.3	0.13	2.97
680	0.26	0.11	3.02

In a previous article we showed that square wave voltammetry is valid for the analysis of reversible system with the formation of a solid phase on condition that the current density of the peak, δi, is linear with the frequency of the waveform signal [20]. The relationship is [21]:

$$\delta i = nFC_0 \frac{1-\Gamma}{1+\Gamma}\sqrt{\frac{Df}{\pi}} \tag{5}$$

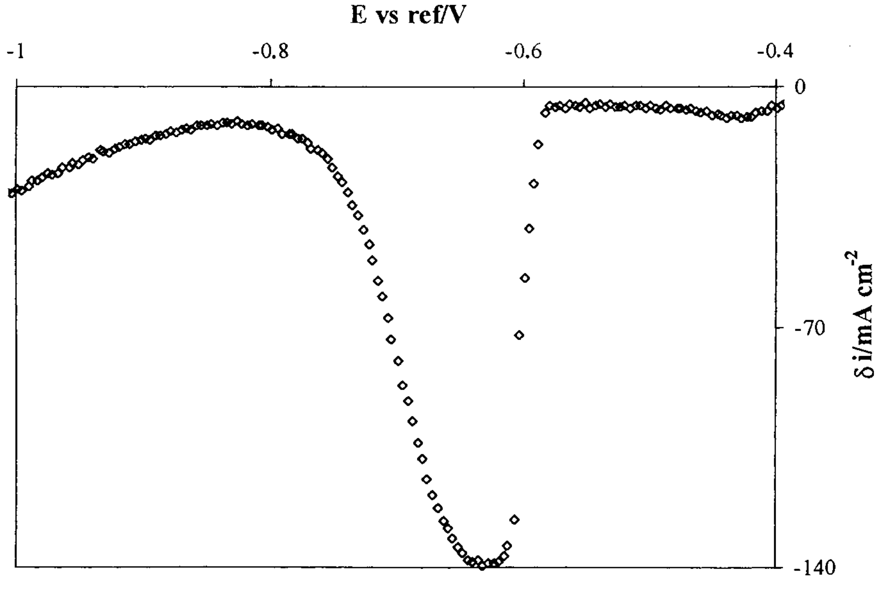

Fig. 8. S. W. Voltammogram of NaCl–KCl–UCl_3 [U] = 1.5 mass %, θ = 715 °C, frequency 16 Hz. Working electrode W; comparison electrode Pt.

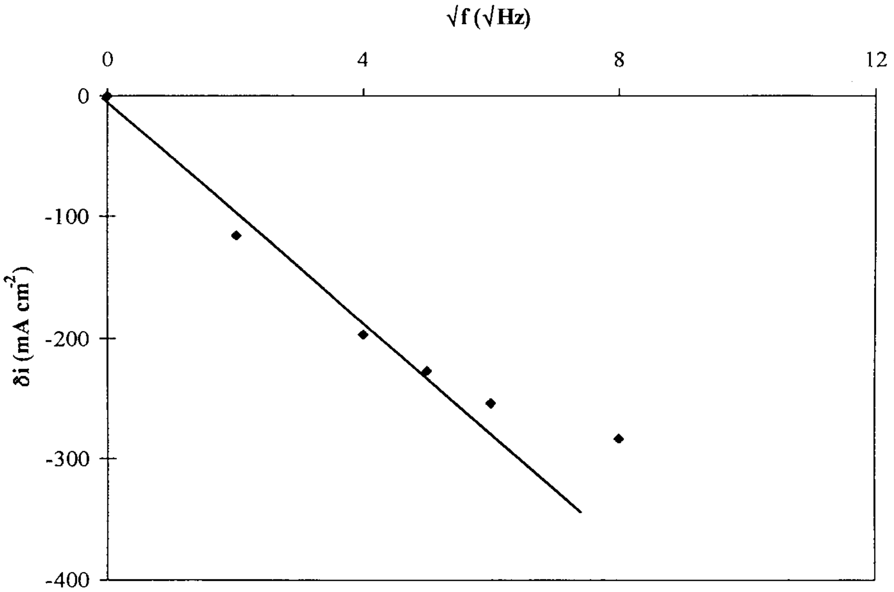

Fig. 9. Reduction peak differential current density for U^{III} species against square wave frequency in square wave voltammetry, $\theta = 715\,°C$, [U] = 1.5 mass %. Working electrode W; comparison electrode Pt.

with $\Gamma = \exp(nF\Delta E/2RT)$. ΔE is the amplitude of the square wave potential.

Figure 9 shows that this relation holds for frequencies less than 25 Hz. The signal was deconvoluted by taking into account the second part of the peak (Figure 10). The measured midpeak width at midheight ($W_{1/2}/2$) must obey the following equation [10, 15] on condition that the potential pulses are low:

$$\frac{W_{1/2}}{2} = \frac{3.52\,RT}{2nF} \tag{6}$$

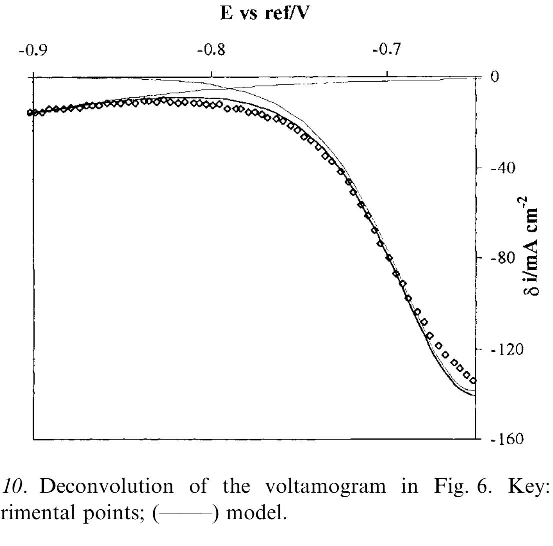

Fig. 10. Deconvolution of the voltamogram in Fig. 6. Key: (◇) experimental points; (———) model.

The best agreement between the model and the experimental points (Figure 10) is obtained when *n*, the number of exchanged electrons, is 3.

Now, it is possible to conclude that peak IIc is associated with the reduction of U(III) to uranium metal in a single step with an exchange of three electrons, since all the electrochemical methods used to analyse this step are in agreement on this point.

3.4. *Determination of the diffusion coefficient of U(*III*)*

A series of cyclic voltammograms was obtained at several temperatures in order to calculate the diffusion coefficient of U(III), *D*, at each value of *T*, using Equation 3. The plot of $\log D$ against $1/T$ is shown in Figure 11. The slope of the straight line and the value of *D* on the *y* axis allows the following equation to be proposed:

$$D = 0.022 \exp\left(\frac{-5867}{T}\right)$$

where *T* is in K and *D* in cm^2 s^{-1}.

The expression for *D* can be verified using the other electrochemical methods:

(i) by chronopotentiometric measurement, in Table 4 following Sand's equation (Equation 4).
(ii) by square wave voltammetry, by plotting the current peak versus $\sqrt{f}$, (Figure 9 and Equation 5).

The values of the diffusion coefficient *D* given by the three methods at $\theta = 715\,°C$ are reported in Table 5 and they show good agreement.

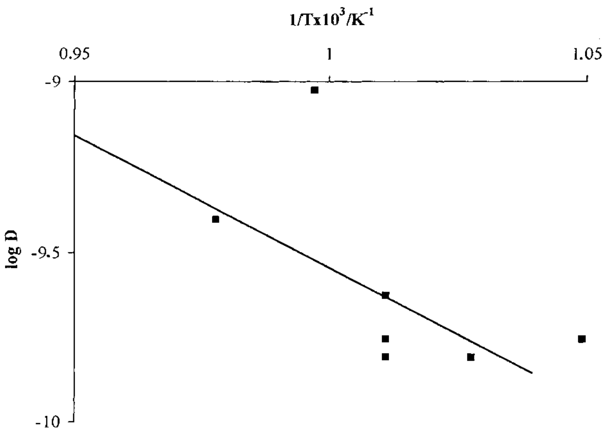

Fig. 11. Linear relation between log D and $1/T$. Working electrode W; comparison electrode Pt.

Table 4. Value of the diffusion coefficient of U(III) calculated by chronopotentiometry

C/mol cm^{-3}	$i\tau^{1/2}/C$/A cm s$^{1/2}$ mol^{-1}	D/cm^2 s^{-1}
9.0×10^{-5}	1.9×10^3	5.6×10^{-5}
8.0×10^{-5}	1.75×10^3	4.7×10^{-5}
6.8×10^{-5}	1.9×10^3	5.6×10^{-5}

θ = 716 °C.

Table 5. Values of the diffusion coefficient of U(III) in NaCl–KCl at 715 °C obtained with three different methods

Method used	Cyclic voltammetry	Chronopotentiometry	Square wave voltammetry
D/cm^2 s^{-1} θ = 715 °C	5.8×10^{-5}	5.6×10^{-5}	5.3×10^{-5}

4. Conclusion

This paper gives preliminary results on the electrochemical mechanism followed by trivalent uranium ions leading to cathodically-deposited uranium crystals.

We observed that the cathodic polarization of U^{III} promotes two competitive reactions over the same potential range: (i) electrodeposition of uranium, (ii) formation of a subhalide compound of uranium (U^I). Metallic uranium is obtained in a single step reduction: $U^{III} + 3\,e^- \rightarrow U$ which is reversible and controlled by the mass transport of the electrolyte; the values of the diffusion coefficient of U^{III} measured by different electrochemical techniques were very similar.

The competitive reaction, observed in the cyclic voltammograms either as a ‘prepeak’ or a ‘postpeak’, depending on the cathode material, is irreversible and leads to a surface compound, U^I which is insoluble and probably adsorbed on the cathode. This reaction is not controlled by the diffusion of the electrolyte; therefore, high concentrations of U^{III} would minimise its importance, compared to uranium formation.

Acknowledgements

The authors express their thanks to the C.R.V. Pechiney Company and, in particular, S. Bouvet and I. Ronga, for their collaboration and support in this research.

References

1. M.V. Smirnov and O.V. Skiba, *Electrochem. Molten and Solid Electrolytes* **2** (1964) 12.
2. G. Boisde, G. Chauvin, H. Coriou and J. Hure, *Electrochim. Acta* **5** (1961) 54.
3. S. Flengas, *Can. J. Chem.* **39** (1961) 773.
4. B. Partridge, *J. Inorg. Nucl. Chem.* **19** (1961) 379.
5. M.V. Smirnov and O.V. Skiba, *Trans. Inst. Electrochem.* **2** (1964) 1.
6. O.V. Skiba, M.V. Smirnov and T.F. Khazemova, *Electrochem. Molten and Solid Electrolytes* **2** (1964) 7.
7. D.L. Hill, J. Perano and R.A. Osteryoung, *J. Electrochem. Soc.* **107** (1960) 698.
8. F. Caligara, L. Martinot and G. Duyckaerts, *Bull. Soc. Chim. Belg.* **75** (1967) 15.
9. D.S. Poa, Z. Tomczuk and R.K. Steunenberg, *J. Electrochem. Soc.* **135** (1988) 1161.
10. P. Chamelot, B. Lafage and P. Taxil, *J. Electrochem. Soc.* **143**(5) (1996) 1570.
11. R.J. Gale and D.G. Lovering, ‘Molten Salt Techniques’ (Plenum Press, New York, 1984), p. 152.
12. A.T. Hubbard and F.C. Anson, *Anal. Chem.* **38** (1966).
13. C.R. Christensen and F.C. Anson, *Anal. Chem.* **35** (1963).
14. L. Martinot, *J. Inorg. Nucl. Chem.* **37** (1978) 2525.
15. A.J. Bard and R.L. Faulkner, ‘Electrochimie: Principes, Methodes et Applications’ (Masson, Paris, 1983).
16. H.J.S. Sand, *Phil. Mag.* **1** (1901) 45.
17. J.G. Osteryoung and J.J. O’Dea, *Electroanal. Chem.* **14** (1986) 209.
18. B.N. Kabanov, ‘Electrochemistry of Metals and Adsorption’ (Freund Publishing House, Israel, 1969), p. 3.
19. E. Laviron, *Electroanal. Chem. Interfac. Electrochem.* (Elsevier Sequoia S.A., Lausanne), **52** (1974) 355.
20. P. Chamelot, B. Lafage and P. Taxil, *Electrochim. Acta* **43** (5–6) (1997) 607.
21. G.C. Barker, *Anal. Chim. Acta* **18** (1958) 118.